

Granular Packings and Fault Zones

J. A. Åström,¹ H. J. Herrmann,² and J. Timonen¹

¹*Department of Physics, University of Jyväskylä, P.O. Box 35, FIN-40351 Jyväskylä, Finland*

²*ICAI, University of Stuttgart, Pfaffenwaldring 27, D-70569 Stuttgart, Germany*

(Received 16 March 1999; revised manuscript received 24 August 1999)

The failure of a two-dimensional packing of elastic grains is analyzed using a numerical model. The packing fails through formation of shear bands or faults. During failure there is a separation of the system into two grain-packing states. In a shear band, local “rotating bearings” are spontaneously formed. The bearing state is favored in a shear band because it has a low stiffness against shearing. The “seismic activity” distribution in the packing has the same characteristics as that of the earthquake distribution in tectonic faults. The directions of the principal stresses in a bearing are reminiscent of those found at the San Andreas Fault.

PACS numbers: 45.70.Cc

There are different natural systems which fail through a localized failure in narrow shear zones. These so-called shear bands appear, for example, in granular packings [1,2]. Tectonic faults are another example of shear failure in narrow zones. The objective of this Letter is to demonstrate similarities between these two systems, and to show that granular packings may provide a significant contribution to understanding the mechanics of tectonic faults.

We investigate a two-dimensional packing of elastic spheres [3]. To avoid a perfectly regular packing there is a random variation in the radii of the spheres, $0.25 \leq r \leq 0.75$. In a tectonic fault the spheres would correspond to discrete pieces of cracked rock within the Earth’s crust. We imagine that a fault is approximately invariant in the vertical direction and may therefore be considered as two dimensional. The spheres (grains) obey Newton’s mechanics, and there is both a dynamic and a static friction between grains in contact [4]. The static friction is modeled by a spring at the contact. This spring may break (slip) but it is formed again (sticks) at a new contact point after a slip. If the tangential force is larger than $|\mu_s F_n|$, the static friction slips (μ_s is the static friction coefficient and F_n the normal force at the contact). The dynamic friction results in a force $\mu_d F_n$ which acts in the direction that opposes sliding at the contacts. To damp out oscillations in the packing, a “viscous” damping term is introduced. This is just a force proportional to the velocity of a grain, and it acts in the direction opposite to the velocity.

In a tectonic fault the large blocks of rock are, of course, not simple spheres. The most significant difference between a packing of spheres and that of closely packed irregular blocks is that the spheres can rotate on each other as in a bearing. If, however, the shear stress on the blocks in the fault increases, the shape irregularities that hinder the blocks from rotating will eventually break, and blocks will begin to rotate. The introduction of fragmenting blocks is beyond the scope of this investigation, and here we consider only spherical blocks.

At the beginning of a simulation, grains are placed randomly in a two-dimensional box with stiff boundaries. The

packing is then allowed to relax until all velocities vanish. Then the boundary conditions are changed. Stiff horizontal bars at the top and bottom of the packing begin to compress it vertically with a constant velocity. At the sides of the packing “floppy” sheets are attached, and an external pressure P compresses the packing horizontally. Technically this is done by connecting the grains on the sides of the packing by line segments and calculating the forces on the grains as if the line segments were stiff bars under pressure from the outside. The “side grains” consist of all the grains on a side of the packing that can be connected by a chain of line segments whose angles to the vertical never exceed some predefined maximum angle. Since the connections of the side grains are updated often, there is little resistance to local deviations in the shapes of the vertical sides of the packing. The “side sheets” are therefore floppy.

There are several parameters in our model. The geometrical parameters like, e.g., the average radius of the grains are rather trivial. The number of grains is, of course, limited by the computer power. The damping coefficients must be chosen large enough to keep the simulations stable with a reasonable time step, but small enough in relation to the compression velocity. Because of Newton’s second law, the dynamics (i.e., grain accelerations) of the model is invariant as long as the ratio of the contact forces to the mass of the grains stays constant. This means that the scale of the stiffness constants, the pressure P , and the damping coefficients can be chosen freely as long as the mass density of the grains is rescaled accordingly.

Figure 1 shows the result of a simulation. In this particular simulation, Young’s modulus of the grains was 10^{10} N/m², $\mu_s = \mu_d = 0.5$, the mass density of the grains was 10^4 kg/m³, the shear stiffness (static friction) was 2.0×10^9 N/m, and the damping coefficient was 10^4 N s/m. Figure 1A shows the initial packing with the compression bars and the side sheets, while Fig. 1B shows the final configuration of the simulation. Figure 2A shows the traces of the grains during the last part of the simulation. The grains have moved diagonally upwards in

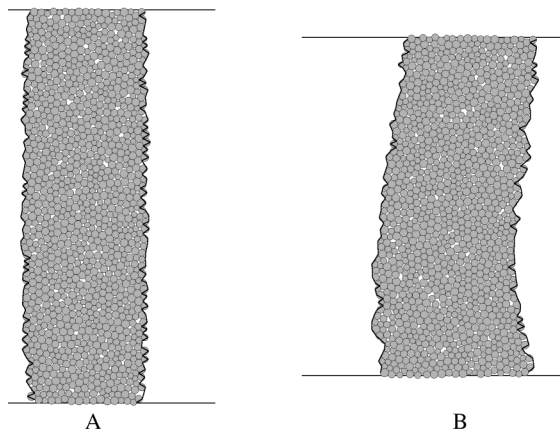


FIG. 1. (A) The initial packing with side sheets and the compression bars. (B) The final packing.

the lower part of the packing and diagonally downwards in the upper part. There are two distinct boundaries in the grain motions. These have been marked by lines. It is only in these two boundary zones that there is significant relative motion between neighboring grains. Shear strain is thus concentrated in these two narrow zones. Figure 2B shows the rotations of the grains during a short time interval. Rotation is indicated by a linear gray scale. Black grains have rotated clockwise (more than 6°), gray grains mean close to zero rotations, while the white ones have rotated counterclockwise (less than -6°). There is a distinct concentration in the shear zones of the grains with the highest rotation rates. The grain motions at the shear zones in Fig. 2A are such that clockwise rotations should be dominant. Figure 2B, however, reveals that both clockwise and counterclockwise rotations are concentrated in both shear zones.

Another surprise appears when one applies the Mohr-Coulomb criterion to the in-plane angle of the failure zones [5]. In the Mohr-Coulomb model the failure zones are assumed to be “slip planes” orientated at the angle that maximizes the difference between the shear force at a grain contact and the force threshold for a contact slip. This

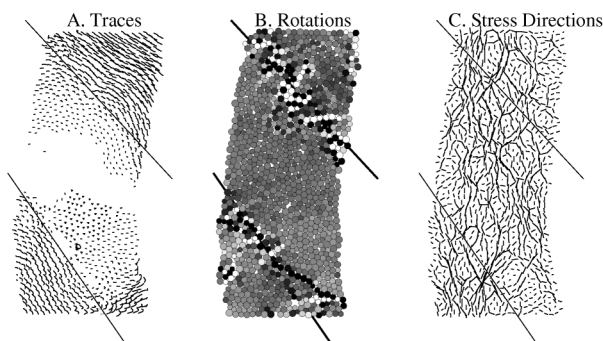


FIG. 2. Traces of the grains, grain rotations (linear gray scale, $\pm 6^\circ$), and principal stress directions. The shear bands are indicated by lines.

predicts a shear-zone angle of about $\pm 32^\circ$ to the vertical. Simulations result in a considerably larger angle, $39^\circ \pm 4^\circ$.

A third surprise appears by examining the stress tensors of the grains. According to elasticity theory, one would expect that the principal stress direction corresponding to the largest eigenvalue of the stress tensors of the grains would be roughly vertical because of the vertical compression of the packing. Large shear stresses would then be induced diagonally in the packing and cause the shear bands according to the Mohr-Coulomb theory. The packing behaves, however, differently. First, the principal directions are not simply vertical but form a network pattern called a “granular skeleton” [6,7] (Fig. 2C). Second, many of the rotating grains in the shear zones have principal stress directions that are almost perpendicular to the zone direction, as seen, for example, in Fig. 3. Quantitatively, we have observed that (20–30)% of the grains in a zone have a principal stress direction that is within 10° from being either parallel or perpendicular to the zone direction. This means that the shear stress on a zone is rather low. This observation is in contrast to the Mohr-Coulomb model, but consistent with field measurements in the San Andreas Fault area [8].

The explanation to the above puzzles can be found on the microscopic level in the geometry of the packing. Figure 4 shows a detail of a shear band. As above, the gray scale indicates the rotations of the grains over a short time interval. In the middle of the figure there is a configuration of about 20 grains in contact that are either black or white, and with only black-white contacts. What this figure shows is a spontaneous formation of a local rotating ball bearing. This configuration can rotate without any shear stress. In areas with dominantly gray grains (i.e., no rotations), the number of contacts and the local density is on the average higher than in the bearing. A perfect bearing can have at most 4 contacts per grain as also seen in Fig. 4A, while a

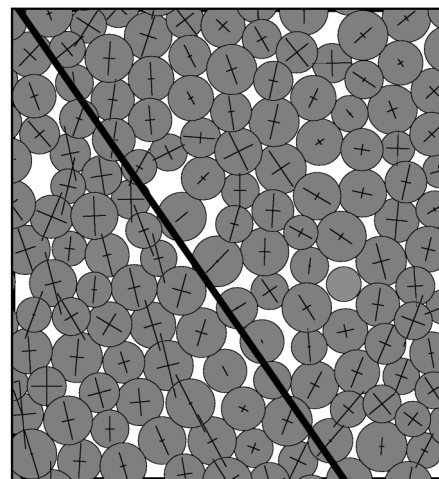


FIG. 3. A detailed picture of the principal stress directions at a shear zone.

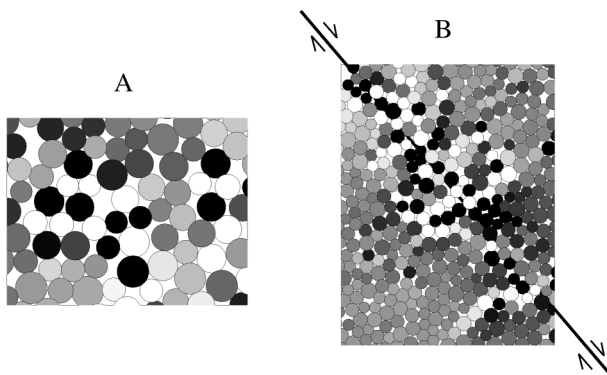


FIG. 4. Detailed pictures of a shear band. The figures are snapshots of the geometry and display the integrated particle rotations over an interval in time as a gray scale. Black corresponds to maximum clockwise rotation, and white the opposite. A perfect rotating bearing containing about 20 grains is visible in A.

dense packing has approximately 6 contacts per grain. The density difference between a perfect bearing and a dense packing is about 15%.

One can think of the local grain configuration as being in one of the two possible “states” separated by an energy barrier. In the “bearing” state the local density of grains is lower, but there is no resistance against shearing. In the “dense packing” state the density is higher, but there is a large resistance against shearing. With this interpretation in mind, Fig. 2B can be seen as a “phase separation” with the bearing state in the shear bands and the dense-packing state elsewhere. This two-state picture does not, of course, work perfectly. The local geometry changes all the time and local bearings form and die as contacts open and close. Sometimes also two or more grains rotate together as a rigid body within a shear band, and sliding contacts are never totally absent. We have detected perfect local bearings of up to about 30 grains which have lived for almost 10% of the total simulation time.

The energy barrier between the two grain-packing states is given by the work against the compression of the packing which is needed to obtain the lower density of the bearing state. The bulk modulus (K) is, in terms of Young’s modulus (E) and Poisson ratio (σ), given by $K = 0.5E/(1 - \sigma)$. On the other hand, the energy gain in the bearing state consists of the relaxation of the shear stress. The shear modulus (μ) is given by $\mu = 0.5E/(1 + \sigma)$. If the density in the bearing state is ρ_b and in the dense packing state ρ_d , we get a critical local shear strain (i.e., the strain at which it is energetically favorable for the system to change state) given by

$$U_c = \sqrt{\frac{1 + \sigma}{1 - \sigma} \frac{\rho_d - \rho_b}{\rho_d}}. \quad (1)$$

The densities in the two states can be approximated by the densities of regular packings in a triangular ($\rho_d = \pi/4$)

and in a square lattice [$\rho_b = \pi/(2\sqrt{3})$]. This gives a numerical value of approximately 0.2 for U_c , which is in reasonable agreement with simulations (the shear bands begin to form when the compressive strain is about 0.1–0.2).

To further test the two-state picture we investigated the average number of contacts per grain as a function of time. The number first increases as a packing is compressed and reaches a maximum of about 5 contacts per grain (this should be compared to a perfect triangular packing for which the number of contacts is 6). When shear bands begin to form, the number decreases by (2–3)%, which corresponds to about 7% of the grains being in the bearing state if we, as above, assume that the number of contacts per grain decreases from 6 to 4 when a grain passes the energy barrier to the bearing state. 7% is a reasonable fraction in comparison with Fig. 2B (where 16.5% of the grains are either black or white).

With this picture in mind it is possible to understand the puzzles mentioned above. The bearings can be formed only when contacting grains rotate in different directions, and therefore there is a concentration of both clockwise and counterclockwise rotations in the shear bands. Since the shear bands are not slip planes the Mohr-Coulomb model is not valid, and it is no surprise that the calculated in-plane angles are not consistent with simulations. Finally, the bearings have no shear stiffness, which means that the principal stress direction will be more or less perpendicular (or parallel) to the shear band, depending on how close to perfect the bearing formation is in the band.

To study the time development of the packing we plot the total volume of the packing as a function of time (Fig. 5a) and the total force on the top compression bar (scaled by the external pressure), also as a function of time

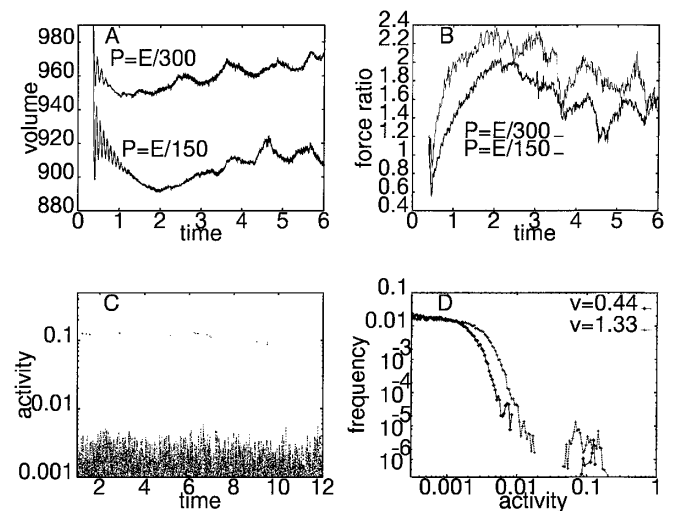


FIG. 5. The total volume (A) and the ratio of the total vertical force to horizontal pressure (B) versus time (the horizontal pressure is $E/150$ and $E/300$, where E is Youngs modulus of the grains). A time series of the force fluctuations (C), and the distribution of the seismic activity (D) (compression velocities 0.44 and 1.33).

(Fig. 5b). The initial volume fluctuations result from the change in the boundary conditions, i.e., from a rigid box to the floppy side sheets. The oscillations are, however, soon damped out. The total volume decreases initially but reaches then a minimum and increases thereafter as bearings begin to form. As expected, a minimum in volume corresponds to a maximum in the total force and vice versa. More interesting than the total force, in relation to tectonic faults, are the fluctuations in the force. The slow energy input due to the compression of the packing is dissipated by the damping, but rapid fluctuations in the force spread through the packing as oscillations, and these can be registered as “seismic activity.” A time series of the activity is shown in Fig. 5c. It clearly shows a distinct separation of the activity into a few large magnitude “earthquakes” and a lot of small-magnitude oscillations. This is also seen in the activity distribution (Fig. 5d) which displays a power-law distribution of the small-magnitude events. There is a distinct gap in the distribution which separates the small magnitude events from the large-size earthquakes. This distribution is qualitatively similar to the characteristic distribution of the seismic activity in fault zones [9].

As mentioned above, the spherical grains used in our numerical model are a simplification in view of a tectonic fault. Asperities on the closely packed fragmented blocks deep in a fault zone will hinder them from rotating. An increasing shear stress will eventually lead to fragmentation of the asperities, and to a release of shear stress which results in earthquakes. For granular packings it has been demonstrated in Refs. [10,11] that fragmentation under a biaxial compression (or a uniaxial compression with periodic boundaries in the other direction) drives a packing towards a space-filling state. It has been found for several fragmentation criteria that the fragment-size distribution approaches a power law of the form $N(r) \propto r^{-2}$, which is fairly close to the size distribution of fractal, space filling, Apollonian packing $N(r) \propto r^{-2.3}$ [12]. It is also possible to build space filling bearings in a similar manner as the Apollonian packing [13]. One can then ask an intriguing question. Could the fragmentation of rocks in tectonic faults lead to the formation of local space filling bearings, and could this explain the extreme weakness to shear deformation of fault zones [14], and could it in some way relate to the appearance of seismic gaps?

In summary, we have demonstrated that local rotating bearings play an important role in shear band formations. The bearing state is favored in shear bands because it significantly reduces shear stiffness. Outside shear bands the packing is denser. Shear band failures lead to a seismic activity distribution that is similar to the characteristic distribution in tectonic fault zones. The reduced shear stiffness in the bearing state leads to a stress orientation that reminds one of that observed at the San Andreas Fault. Fragmentation of blocks in tectonic faults may provide a route to formation of local space-filling bearings which may be connected to the appearance of seismic gaps.

-
- [1] M. Oda, K. Iwashita, and H. Kazama, in *Proceedings of the IUTAM Symposium on Mechanics of Granular and Porous Materials*, edited by N. A. Fleck and C. F. Cocks (Kluwer, The Netherlands, 1997), pp. 353–364.
 - [2] J. P. Bardet, *Mech. Mater.* **18**, 159 (1994).
 - [3] H. Hertz, *J. Reine Angew. Math.* **92**, 136 (1882).
 - [4] J. Schäfer, S. Dippel, and D. E. Wolf, *J. Phys. I (France)* **6**, 5 (1996).
 - [5] See, for example, A. C. Ugural and S. K. Fenster, *Advanced Strength and Applied Elasticity* (Elsevier, London, 1987), pp. 116–118.
 - [6] C. Thornton and G. Sun, in *Numerical Methods in Geotechnical Engineering*, edited by I. Smith (Balkema, Rotterdam, 1994), pp. 143–148.
 - [7] F. Radjai, D. E. Wolf, M. Jean, and J.-J. Moreau, *Phys. Rev. Lett.* **80**, 61 (1998).
 - [8] M. L. Zoback, V. Zoback, J. Mount, J. Eaton, and J. Healy, *Science* **238**, 1105 (1987).
 - [9] S. G. Wesnousky, *Bull. Seismol. Soc. Am.* **84**, 1940 (1994).
 - [10] O. Tsoungui, D. Vallet, J.-C. Charmet, and S. Roux, *C. R. Acad. Sci. Ser. 2* **325**, 457 (1997).
 - [11] J. A. Åström and H. J. Herrmann, *Eur. Phys. J. B* **5**, 551 (1998).
 - [12] K. J. Falconer, *The Geometry of Fractal Sets* (Cambridge University Press, Cambridge, 1985); H. J. Herrmann, G. Mantica, and D. Bessis, *Phys. Rev. Lett.* **65**, 3223 (1990).
 - [13] S. S. Manna and H. J. Herrmann, *J. Phys. A* **24**, 481 (1991).
 - [14] D. Sornette, *Physics Rep.* **313**, 8–11 (1999).